International Journal of Mechanics and Energy (IJME)
Vol. 10, Issue 1, 2023, ISSN: 2286-5845

Modeling of thermal induced phase transformation in NiTi shape memory alloy

Boutheina Ben Fraj[1*], Asma Ben Khalfallah[2], Zoubeir Tourki[2]
[1] *Nanomaterials and Systems for Renewable Energy Laboratory, Research and Technology Center of Energy, Technopole Borj Cedria, Hammam Lif, Tunisia.*
[2] *Mechanical Laboratory of Sousse (LMS), National Engineering School of Sousse ENISo, University of Sousse, Sousse, Tunisia.*

Abstract: The main goal of this research work is to propose a convenient model that describes the evolution of the latent heat during a full transformation cycle and defines the thermal-induced phase transformation behavior of the NiTi shape memory alloy under zero stress conditions. The proposed model is constructed based on experimental data obtained from Differential Scanning Calorimetry (DSC) analyzes, carried out at various cooling/heating rates. The NiTi thermal behavior was studied and modeled across the different temperature ranges of the thermal transformation cycle. The developed constitutive equations were implemented in the Matlab software. The expression of the enthalpy change during both forward and reverse phase transformations was predicted as function of the cooling/heating rate. Moreover, the transformations temperatures were theoretically determined from the proposed model and compared to the experimental ones. A good agreement between experimental and theoretical findings proves that the proposed model provides a precise estimation. The efficiency of the adopted hypotheses is well confirmed.

Key words: Modeling, thermal behavior, phase transformation, transformation temperature, NiTi SMA.

1. Introduction

Shape memory materials are among the smart materials that remain increasingly exploited in high technologies. As a metallic alloy, the NiTi Shape Memory Alloy (SMA) has received much scientific and technological attention in recent decades since it has a distinguished physico-chemical and thermomechanical properties [1-4].

The NiTi SMA has the ability to recover permanent strain by heating above a convinced temperature when undergoing thermomechanical loadings. This behavior is based on a thermoelastic phase transformation called "martensitic transformation" between the austenitic phase (A) at high temperature and martensitic phase (M) at low temperature. This reversible transformation process (A↔M) can be thermally induced, at zero stress, and governed by the transformation temperatures which characterize the beginning and the end of both forward and reverse transformations (A-M) and (M-A), respectively:

- M_s: martensite start temperature at which the austenite begins, under cooling, to transform into martensite: it is the start temperature of the forward thermal-induced transformation (A-M).
- Mf: martensite finish temperature at which the material becomes completely twinned martensite: it is the finish temperature of the forward thermal-induced transformation (A-M).
- A_s: austenite start temperature at which the twinned martensite begins, under heating, to transform into austenite: it is the start temperature of the reverse thermal-induced transformation (M-A).
- Af: austenite finish temperature at which the material returns completely to its mother phase and becomes completely austenite: it is the finish temperature of the reverse thermal-induced transformation (M-A).

These transformation temperatures can be easily determined by thermal analysis [5]. The Differential Scanning Calorimetry (DSC) is the most widely used thermo-analytical analysis to describe the thermal behavior of materials that exhibit phase transformation. This method leads to obtain a heat flow curve as a function of the temperature from which the transformation temperatures, at zero stress, are easily identified (Figure 1). Moreover, the calorimetric analysis provides numerous informations about thermodynamic properties such as transformation heats, enthalpy and entropy [6]. The transformation temperatures depend mainly on the chemical composition [7], heat treatment [8,9], as well as on the microstructural defects [10,11].

The aim of this study consists of modeling the thermal induced phase transformation behavior of the NiTi alloy at zero stress based on our previous experimental results that were obtained for various DSC cooling/heating rates. The thermal behavior is modeled for different temperature ranges. After the identification of the empirical parameters, the transformation temperatures, the

constitutive equations of the proposed model are implemented on the Matlab software in order to compare the theoretical results with the experimental ones.

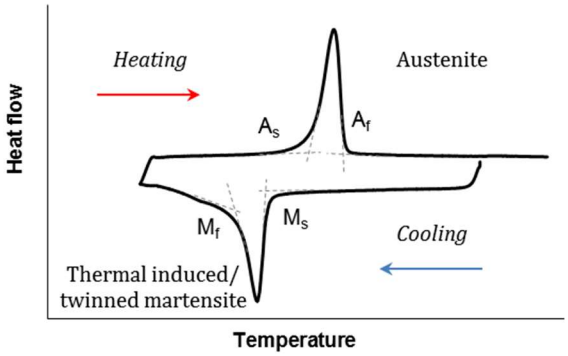

Figure 1. A typical DSC Curve for NiTi SMA.

2. A study of a full thermal phase transformation cycle

In this study, the opted model builds upon the research work of Ortin and Planes [12]. In this model, we consider the thermodynamic characteristics of the thermoelastic martensitic transformation while factoring in the influence of interfaces and interactions between the austenitic and martensitic phases. Additionally, we exclude entropy production resulting from the dissipation of internal work as irreversible heat. Instead, we focus on the internal work that irreversibly dissipates into energy forms other than heat ($dw \geq 0$), which is the significant aspect of our analysis. Furthermore, we assume that the specific heats of both phases are equal. This model presents a more realistic and straightforward approach for practical application.

2.1 Modeling of the forward transformation A-M

– *For T > M_s and For T<M_f*

In this case, the changes in temperature and the motion of austenite grains are involved, which can be quantified in terms of elastic energy. Therefore, the equation for enthalpy change ΔH^{A-M} is as follows:

$$\Delta H^{A-M} = C_p dT + E_{fr} \quad (1)$$

C_p: Specific heat at constant pressure
E_{fr}: Frictional energy

– For M_f< T< M_s

The expression of the internal energy dU as function of temperature is expressed as:

$$dU = TdS + C_v dT - T\bar{d}S \quad (2)$$

C_v: Specific heat at constant volume

We consider that dT or $\dot{T}$ known as the cooling/heating rate is constant [13]:

$$\dot{T} = -\alpha \ (°C\ /min\ ) \quad (3)$$

We can conclude the free enthalpy change is the sum of the elastic energy change (dE_{el}), the frictional energy change (dE_{fr}), the variation of the entropy $(dS)$and the production of the entropy change $(\bar{d}S)$

$$dH = TdS + C_v dT - T\bar{d}S + dE_{fr} + dE_{el} \quad (4)$$

In the following work, we suppose that $\bar{d}S = 0$. This hypothesis means that the transformation occurs without entropy production. It should be noted that $\bar{d}S = 0$ does not mean that the martensitic transformation happens without hysteresis, but the irreversible internal work is not released as heat. The experimental work [12] demonstrates that this approximation holds efficient in more practical scenarios. Based on these assumptions, we can represent the change of free enthalpy as follows:

$$\Delta H^{A-M} = \int_{M_s}^{M_f} T(dS_{A-M}) + \int_{M_s}^{M_f} C_v dT - \int_{M_s}^{M_f} dE_{el} - \int_{M_s}^{M_f} dE_{fr} \quad (5)$$

Where the elastic energy is calculated as:

$$\int_{M_s}^{M_f} dE_{el} = T_0 \int_{M_s}^{M_f} \frac{dQ_M}{T} + \int_{M_s}^{M_f} dQ_M - \int_{M_s}^{M_f} dE_{fr} \quad (6)$$

T_0: equilibrium temperature
Q_M: Transformation heat during A-M transformation
The adopted entropy argument is:

$$\Delta S_{A-M} = \int_{M_s}^{M_f} \frac{dQ_M}{T} \quad (7)$$

The frictional work during the forward martensitic transformation is defined as:

$$\int_{M_s}^{M_f} dE_{fr} = \left(\frac{A_f - M_s}{2}\right) \Delta S_{A-M} \quad (8)$$

So, the final expression of ΔH^{A-M} is:

$$\Delta H^{A-M} = \int_{M_s}^{M_f} T(dS_{A-M}) + \int_{M_s}^{M_f} C_v dT - T_0 \int_{M_s}^{M_f} \frac{dQ_M}{T} - \int_{M_s}^{M_f} dQ_M \quad (9)$$

2.2 Modeling of the reverse transformation M-A

– For T < A_s and for For T> $\boldsymbol{A_f}$

The equation of enthalpy change ΔH^{M-A} is as follows:

$$\Delta H^{M-A} = C_p(dT) + E_{fr} \quad (10)$$

– For A_s<T<A_f

$$\Delta H^{M-A} = \int_{A_s}^{A_f} T(dS) + \int_{A_s}^{A_f} C_v dT - \int_{A_s}^{A_f} dE_{el} + \int_{A_s}^{A_f} dE_{fr} \quad (11)$$

The elastic energy can be expressed in the same way as:

$$\int_{A_s}^{A_f} dE_{el} = T_0 \int_{A_s}^{A_f} \frac{dQ_A}{T} + \int_{A_s}^{A_f} dQ_A - \int_{A_s}^{A_f} dE_{fr} \quad (12)$$

Q_A: Transformation heat during M-A transformation

In order to simplify the calculation, the frictional energies during the forward and the reverse transformations are considered equal:

$$\int_{A_s}^{A_f} dE_{fr} = \int_{M_s}^{M_f} dE_{fr} = \left(\frac{A_f - M_s}{2}\right) \Delta S_{A-M} \quad (13)$$

Thus, the final expression of ΔH^{M-A} is:

$$\Delta H^{M-A} = \int_{A_s}^{A_f} T(dS_{M-A}) + \int_{A_s}^{A_f} C_v dT - T_0 \int_{A_s}^{A_f} \frac{dQ_A}{T} - \int_{A_s}^{A_f} dQ_A + (A_f - M_s)\Delta S_{A-M} \quad (14)$$

2.3. Implementation and comparison with experimental results

In our previous studies on NiTi SMA thermal behavior [5,14], a full free stress thermal cycle was carried out through DSC analyzes. The experiments were performed at different cooling/heating rates in order to understand its effect on the thermal properties of NiTi alloy. Figure 2 illustrates the DSC curves of the NiTi samples (annealed at 650°C for 1 hour) as function of cooling/heating rate, varying from 5°C/min to 20°C/min. In the course of cooling the specimen, the forward (A-M) transformation is observed to be exothermic. However, during heating, the reverse (M-A) transformation presents an endothermic reaction.

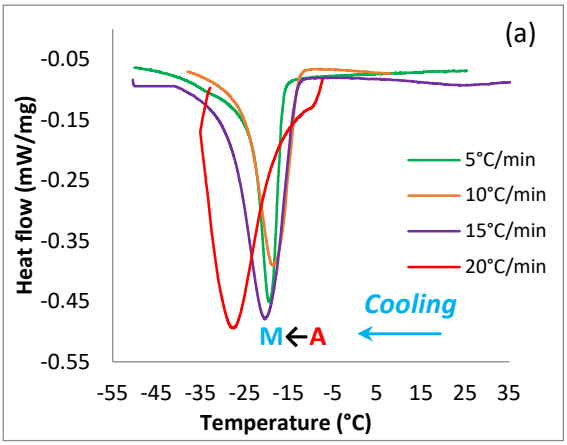

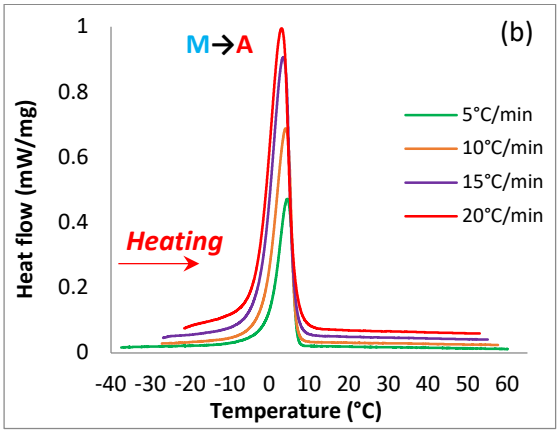

Figure 2. The NiTi DSC curves obtained at different cooling/heating rates; (a) during cooling process, (b) during heating process.

In order to validate the proposed model and compare theoretical and experimental results, Matlab software was used to implement the heat flow as a function of temperature. The resulted equation system is as shown below:

$$\begin{cases} \text{Forward} \begin{cases} C_p dT \ ; \text{For T} > \text{M}_\text{s} \\ \int_{M_s}^{M_f} T(dS_{A-M}) + \int_{M_s}^{M_f} C_v dT - T_0 \int_{M_s}^{M_f} \frac{dQ_M}{T} - \int_{M_s}^{M_f} dQ_M \ ; \ for \ \text{T} \in [\text{M}_\text{s}, \text{M}_\text{f}] \\ C_p dT; \ \text{For T} < \ \text{M}_\text{f} \end{cases} \\ \text{Reverse} \begin{cases} C_p dT; \ For \ \text{T} < \ \text{A}_\text{s} \\ \int_{A_s}^{A_f} T(dS_{M-A}) + \int_{A_s}^{A_f} C_v dT - T_0 \int_{A_s}^{A_f} \frac{dQ_A}{T} - \int_{A_s}^{A_f} dQ_A + (A_f - M_s)\Delta S_{A-M} \ ; for \ \text{T} \in [\text{A}_\text{s}, \text{A}_\text{f}] \\ C_p dT \ ; \text{For T} > \ \text{A}_\text{f} \end{cases} \end{cases} \quad (15)$$

2.3.1 Resolution system

Based on the experimental results, the values of the different parameters were determined and serve as input for the Matlab program (Table 1). The transformation heats (absorbed and released) Q_A and Q_M are calculated as the area of the peak of the DSC curve delimited by the base line [13]. Theoretically, Q_A and Q_M can be expressed as a cosine function [15]:

$$Q_A = H_A * \cos\left[a_A\left(T - A_p\right)\right] + C_v \quad (16)$$

$$Q_M = H_M * \cos\left[a_M\left(T - M_p\right)\right] + C_v \quad (17)$$

Where:

- H_A/H_M: The peak amplitude of the experimental DSC curve, during the reverse/forward phase transformation.
- a_A / a_M: Constant used for the plot of the peak corresponding to Q_A and Q_M.
- A_p/M_p: The peak temperature of the DSC curve during the forward/reverse transformation path.

$$A_p = \frac{A_f + A_s}{2} \quad (18)$$

$$M_p = \frac{M_f + M_s}{2} \quad (19)$$

Q_e: The experimental value of the absorbed heat during the reverse transformation.

T_0: Equilibrium temperature

$$T_0 = \frac{M_s + A_f}{2} \quad (20)$$

T_0': Characteristic temperature

$$T_0' = \frac{M_f + A_s}{2} \quad (21)$$

We integrate the expression of the absorbed heat during the reverse transformation between the austenitic temperatures: A_s and A_f. Consequently, a system of two equations will be created:

$$\begin{cases} \int_{A_s}^{A_f} Q_A = Q_e \\ A_p = \frac{A_f + A_s}{2} \end{cases} \quad (22)$$

Then, we find the values of A_s and A_f.

Using the expressions (20) and (21) of T_0 and T_0', respectively, we can easily determine the values of $M_s$and M_f.

$$M_s = 2 * T_0 - A_f \quad (23)$$

$$M_f = 2 * T_0' - A_s \quad (24)$$

Table 1. Input values of experimental data for various cooling/heating rates

α (°C/min)	H_{M-A} (mJ/mg)	a_A (°C^{-1})	A_p (°C)	Q_e (mJ/mg)	T$_0$' (°C)	T$_0$ (°C)	H_{A-M} (mJ/mg)	a_M (°C^{-1})	M_p (°C)
5	5.69	0.5	2.87	50.45	-11.48	-4.55	-5.37	-0.5	-18
10	8	0.5	2.24	75.85	-14.47	-3.69	-4.7	-0.3	-20.36
15	11	0.27	1.57	119.42	-16.34	-3.64	-6	-0.15	-21.55
20	12	0.27	1.36	159.86	-19.71	-4.97	-5.9	-0.2	-21.55

2.3.2 Results and discussion

The results of the proposed model are limited to the determination of the transformation temperatures during both forward and reverse phase transformations. Table 2 allows the comparison

between the experimental results and the theoretical predicted values of the transformation temperatures.

The obtained values are plotted in Figure 3 which illustrate their dependence on the DSC cooling/heating rate.

Table2. Comparison between experimental and theoretical values of the transformation temperatures for various cooling/heating rates

α=5 °C/min	A_s (°C)	A_f (°C)	M_s (°C)	M_f (°C)
Experimental	-0.96	6.7	-16.23	-23.18
Theoretical	-0.34	6.08	-15.18	-22.61
α=10 °C/min	A_s (°C)	A_f (°C)	M_s (°C)	M_f (°C)
Experimental	-2.43	6.82	-14.20	-26.52
Theoretical	-0.99	5.47	-12.85	-27.95
α=15 °C/min	A_s (°C)	A_f (°C)	M_s (°C)	M_f (°C)
Experimental	-3.42	6.56	-13.85	-29.26
Theoretical	-4.37	7.51	-14.80	-28.30
α=20 °C/min	A_s (°C)	A_f (°C)	M_s (°C)	M_f (°C)
Experimental	-4.25	6.97	-16.91	-35.18
Theoretical	-4.51	7.23	-17.17	-34.91

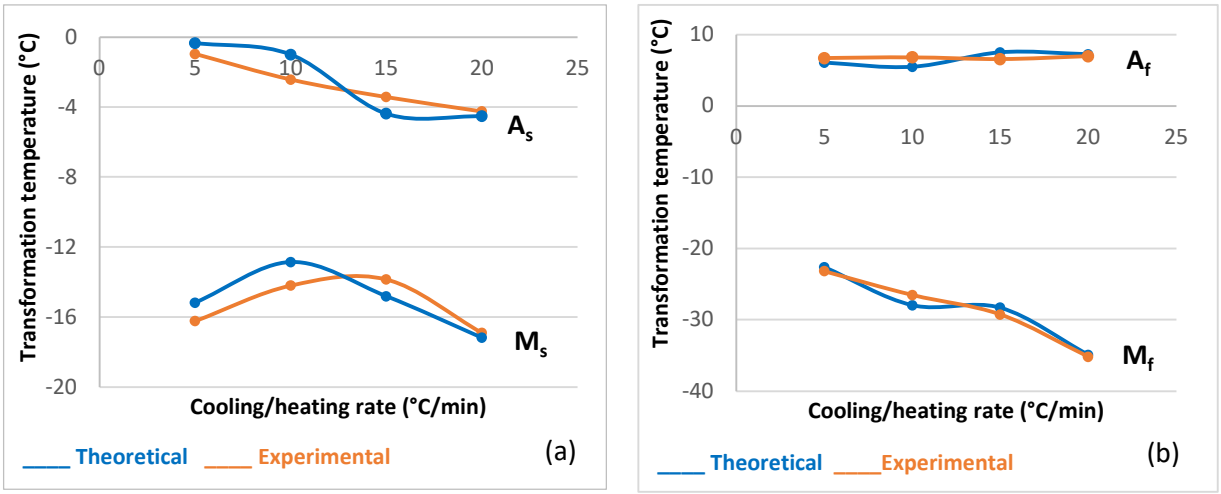

Figure 3. The variation of theoretical and experimental values of transformation temperatures as function of cooling/heating rate; (a) start temperatures (As and Ms) and (b) finish temperatures (Af and Mf).

It is clearly seen that the theoretical values are close to those determined from the calorimetric experiments, mainly for the temperature Mf. The small difference in values may be due to the

simplified hypothesis used in the proposed model. It can be also be caused by the Matlab resolution and the initial solution taken to solve the equation system. The observed coherence between experimental and the theoretical results proves that the proposed model can be considered as a reliable one, since it is in good agreement with the experimental study.

3. Conclusion

The main purpose of this study was to propose a model describing the heat flow evolution as function of temperature and DSC cooling/heating rate, during a thermal induced phase transformation of a NiTi shape memory alloy. For different temperature ranges, the resolution system was presented and the constitutive equations were implemented using Matlab software. The transformation temperatures were theoretically determined based on the proposed model and compared with the experimental ones, extracted from the DSC analyses. An excellent agreement between experimental and predicted values proves that the developed model estimate accurately the transformation temperatures which are considered as the key thermal property of the NiTi phase transformation behavior.

References

[1] Iskender O, Mehmet AK, Ece K, Canan AC, Kemal A (2019) Shape memory alloys phenomena: classification of the shape memory alloys production techniques and application fields. Eur. Phys. J. Plus. https://doi.org/10.1140/epjp/i2019-12925-2

[2] Jithin MA, Sidhila PS, Udayashankar NK (2022) Pulse frequency effect on the NiTi plasmas characteristics and thin film properties and fabrication of NiTi micro-comb structures. Mater Today: Proc. https://doi.org/10.1016/j.matpr.2022.05.418

[3] Joula M, Dilibal S, Mafratoglu G, Danquah JO, Alipour M (2022) Hybrid Battery Thermal Management System with NiTi SMA and Phase Change Material (PCM) for Li-ion Batteries. Energies. https://doi.org/10.3390/en15124403

[4] Chikhareva M, Vaidyanathan R (2023) A Thermal, Mechanical, and Materials Framework for a Shape Memory Alloy Heat Engine for Thermal Management. Nanomaterials. https://doi.org/10.3390/nano13152159

[5] Ben Fraj B, Gahbiche A, Zghal S, Tourki Z (2017) On the Influence of the Heat Treatment Temperature on the Superelastic Compressive Behavior of the Ni-Rich NiTi Shape Memory Alloy. J. Mater. Eng. Perform. https://doi.org/10.1007/s11665-017-2974-2

[6] Fraj, B.B., Zghal, S., Tourki, Z. (2018). DSC Investigation on Entropy and Enthalpy Changes in Ni-Rich NiTi Shape Memory Alloy at Various Cooling/Heating Rates. In: Haddar, M., Chaari, F., Benamara, A., Chouchane, M., Karra, C., Aifaoui, N. (eds) Design and Modeling of Mechanical Systems—III. CMSM 2017. Lecture Notes in Mechanical Engineering. Springer, Cham. https://doi.org/10.1007/978-3-319-66697-6_61.

[7] Balci E, Dagdelen F, Mohammed SS, Ercan E (2022) Corrosion behavior and thermal cycle stability of TiNiTa shape memory alloy. J Therm Anal Calorim. https://doi.org/10.1007/s10973-022-11697-7

[8] Teixeira R, Freitas Rodrigues P, Baptista Ribeiro S, Dos Santos P (2021) The influence of aging treatment on the microstructural and mechanical behavior by ultra-micro hardness tester in Ni-rich NiTi alloy. Cadernos UniFOA, Volta Redonda (RJ). https://doi.org/10.47385/cadunifoa.v16.n47.3810

[9] Jan D, Łukasz R, Damian K, Jakub K, Marek SW, Krzysztof K, Piotr S, Hubert D, Bogdan A, Eduard C (2022) Microstructure, Mechanical Properties, and Martensitic Transformation in NiTi Shape Memory Alloy Fabricated Using Electron Beam Additive Manufacturing Technique. JMEPEG. https://doi.org/10.1007/s11665-021-06241-x

[10] Chowdhury P, Patriarca L, Ren G, Sehitoglu H (2016) Molecular dynamics modeling of NiTi superelasticity in presence of nanoprecipitates. Inter. J. Plas. https://doi.org/10.1016/J.IJPLAS.2016.01.011

[11] Cirstea CD, Karadeniz-Povoden E, Kozeschnik E, Lungu M, Lang P, Balagurov A, Cirstea V (2017) Thermokinetic Simulation of Precipitation in NiTi Shape Memory Alloys. IOP Conf. Series: Mater. Sci. Eng. https://doi.org/10.1088/1757-899X/209/1/012057

[12] Ortin, J., and Antoni Planes (1989) Thermodynamics of thermoelastic martensitic transformations, Acta Metallurgica, vol. 37(5), 1433-1441.

[13] Resnina, Natalia, and Sergey Belyaev (2015) Entropy change in the B2-> B19'martensitic

transformation in TiNi alloy, Thermochimica Acta,. https://doi.org/10.1016/j.tca.2015.01.004

[14] Ben Fraj Boutheina and Tourki Zoubeir, Influence of cooling and heating rates on the thermal properties of Ni-Ti shape memory alloy, in International Federation of Heat Treatment and Surface Engineering, Savannah, Georgia, USA, April 18–21, 2016,481-486

[15] Zhang, Jian-Jun, Yue-Hong Yin, and Jian-Ying Zhu. (2013) Electrical resistivity-based study of self-sensing properties for shape memory alloy-actuated artificial muscle., Sensors,2013, vol. 13.10, 12958-12974. https://doi.org/10.3390/s131012958